

Interactive comment on “Solubility and reactivity of HNCO in water: insights into HNCO’s fate in the atmosphere” by N. Borduas et al.

Anonymous Referee #1

Received and published: 7 October 2015

Summary and General Comments: Borduas and coworkers report on a series of laboratory experiments designed to constrain the effective Henry’s law coefficient for HNCO at a range of atmospherically relevant pH. Further, the authors determine the hydrolysis lifetime of HNCO as a function of pH and temperature for three known hydrolysis mechanisms. The paper is well written, systematic, and will have impact on the community. This paper should be published following the authors attention to a few comments.

Specific Comments:

Page 24218 Line 24: The study of isocyanates from an environmental perspective predates the work of Roberts. Some specific examples include the Bhopal Disaster in India. Perhaps a line on this in the introduction is worthwhile?

This paper is based on the study of the HNCO molecule, whereas it was methyl isocyanate that was leaked out during the Bhopal, India disaster. We prefer not to include the discussion of the Bhopal Disaster in our introduction as it is not directly relevant to HNCO. No changes to the manuscript were made.

Page 24221 Line 6: Where are Reactions 1-3? They were listed in the abstract, but should be included in the main text.

They are presented in Scheme 1.

Page 24221: It would be interesting to note what additional condensed phase reactions involving HNCO are potentially important. Is there any indication that NCO- reactions with condensed phase organics are important to atmospheric chemistry?

We believe that the condensed phase reactive form of isocyanic acid is in its protonated form, i.e. HNCO. The conjugate base, NCO-, is a poor electrophile as well as a poor nucleophile and consequently is expected to be somewhat stable under ambient particle conditions. Page 24233 lines 13-15 addresses the reviewer’s point on other potential reactions with HNCO and we added that these nucleophiles may be amines and alcohols.

The sentence now reads, “There is also the possibility that HNCO has other currently unknown sinks in cloud water that may be competitive with its hydrolysis and further work on HNCO’s aqueous phase chemistry with nucleophiles such as amines and alcohols is currently underway in our laboratories.”

Page 24222 Line 12: It is noted that 10 ions were tracked, although the manuscript discusses only NCO- (and indirectly acetate ion). What other ions were measured, and why? Were any other acids expected (or measured) in the system.

Other ions measured included m/z 59 (CH_3COO^-), m/z 119 ($(\text{CH}_3\text{COOH})\text{CH}_3\text{COO}^-$), m/z 51 (dark counts), m/z 35 (Cl^-), m/z 45 (HCOOH , as HCOO^-), m/z 46 (HONO , as NO_2^-), m/z 96, m/z 102 and m/z 113. None of these ions was observed to change during the experiments and they were monitored to ensure the CIMS was operating correctly. This list of ions was added to the text after line 12.

The manuscript now reads, "Ions measured included m/z 59 (AcO^-), m/z 119 ($(\text{AcOH})\text{AcO}^-$), m/z 51 (black counts), m/z 35 (Cl^-), m/z 42 (NCO^-), m/z 45 (HCOO^-), m/z 46 (ONO^-), m/z 96, m/z 102 and m/z 113. For the exception of m/z 42, none of the ions were observed to change during the experiments."

Page 24222: Is there an absolute humidity dependence on the sensitivity to NCO^- that needs to be accounted for when changing the flow rate over the water solutions? Or is the NCO^- sensitivity not dependent on absolute water concentration (or the analysis independent of this effect if it existed).

The reviewer raises a good point. Previous work suggests that there is no significant role of water vapour in HNCO 's detection by acetate CIMS (Roberts et al. 2010), and so we did not investigate the RH dependence of HNCO . In addition, we had a N_2 dilution flow for the inlet of the CIMS and thus was detecting HNCO under conditions of $< 20\%$ RH.

We added these clarifications in the text, "Previous work suggests there is no significant role of water vapour in HNCO 's detection by acetate CIMS (Roberts et al. 2010). With the CIMS's inlet dilution, the RH within the ion molecule region was $< 20\%$."

Page 24223 Line 12: Perhaps provide reference to one of the earlier Roberts papers (or perhaps even earlier in the literature) that first sublimed cyanuric acid as a HNCO calibration source.

Agreed. We have added the Belson and Strachan 1982 and Roberts et al. 2010 references to line 12.

References:

Roberts, J. M., Veres, P., Warneke, C., Neuman, J. A., Washenfelder, R. A., Brown, S. S., Baasandorj, M., Burkholder, J. B., Burling, I. R., Johnson, T. J., Yokelson, R. J. and de Gouw, J.: Measurement of HONO , HNCO , and other inorganic acids by negative-ion proton-transfer chemical-ionization mass spectrometry (NI-PT-CIMS): application to biomass burning emissions, *Atmos. Meas. Tech.*, 3, 981-990, 2010.

Interactive comment on “Solubility and reactivity of HNCO in water: insights into HNCO’s fate in the atmosphere” by N. Borduas et al.

Anonymous Referee #2

Received and published: 6 October 2015

This paper discusses the measurements of the effective Henry’s law constant and true Henry’s law constant for HNCO by acetate ion CIMS, as well as the hydrolysis rate constants for the three decomposition pathways of HNCO using ion chromatography. Additionally, they determine the pH dependence and temperature dependence of these parameters and use this information to determine the likely lifetime of HNCO over a range of atmospherically-relevant temperatures, pH values, and aerosol/fog/cloud liquid water contents. They find that based on their measurements, the lifetime of HNCO will likely be a longer-lived species than previously thought and exposure might be higher than previously predicted. I found this to be a nicely-written, very thorough paper and recommend that it be published in ACP after addressing the minor comments below.

Comments:

Abstract: The effective Henry’s law constant is more atmospherically-relevant than the true Henry’s law constant because it encompasses any additional solubility due to the ability of HNCO to possibly hydrate, and to dissociate in the aqueous phase. Therefore, K_{Heff} should be given in the abstract either instead or in addition to K_{H} .

Agreed. In addition to K_{H} , $K_{\text{H}}^{\text{eff}}$ is now also given at 298 K and pH3. We thank the reviewer for this recommendation.

The abstract now reads, “By conducting experiments at different pH values and temperature, a Henry’s Law coefficient K_{H} of $26 \pm 2 \text{ M atm}^{-1}$ is obtained, with an enthalpy of dissolution of $-34 \pm 2 \text{ kJ mol}^{-1}$, which translates to a $K_{\text{H}}^{\text{eff}}$ of 31 M atm^{-1} at 298 K and at pH 3.”

Equation 1: The effective Henry’s law constants for small aldehydes such as glyoxal and methylglyoxal incorporate the fact that the carbonyl groups can hydrate to diol groups. HNCO also has such a carbonyl group so the authors may wish to consider that there may be additional processes beyond just pH dependence that determine K_{Heff} .

HNCO has two π -bond systems and so its reactivity is different than a carbonyl group. In fact, water reacts with HNCO irreversibly rather than form diols like aldehydes (see page 24221, line 4). Once water adds to the C in HNCO, carbamic acid is formed which then decomposes to NH_3 and CO_2 .

Section 2.1: A very brief overview paragraph with an overview of the experimental work should be added here prior to section 2.1.1. This will provide some context for the “The CIMS was built in house :” sentence of section 2.1.1.

Good suggestion! A one sentence description was added, which reads, “To measure the effective Henry’s Law coefficient $K_{\text{H}}^{\text{eff}}$ of HNCO, we use a bubbler column experimental set

up and detect HNCO through chemical ionization mass spectrometry.” We also did the same for section 2.2.1.

Section 2.1.1: Are the detection limits and sensitivity of HNCO known for acetate CIMS? Why was the acetic anhydride flow passed through a Po-210 radioactive source? You mention that the CIMS monitored 10 m/z values, and then later say that NCO⁻ is detected at m/z 42. Were other m/z values monitored, and if so which ones and why?

Detection limits and sensitivities for HNCO will depend on the CIMS instrument used. For this work, we did not need to calibrate for HNCO as we report relative kinetics. Background HNCO counts are about 5×10^{-4} ncps, whereas we were operating at HNCO signals ~ 0.1 ncps. (The background counts were added to the text on page 24223, line 16.)

Acetic anhydride was passed through a Po-210 radioactive source to generate AcO⁻, the reagent ion. This reason was added to the sentence in the text.

Other ions measured included m/z 59 (CH₃COO⁻), m/z 119 ((CH₃COOH)CH₃COO⁻), m/z 51 (black count), m/z 35 (Cl⁻), m/z 45 (HCOOH), m/z 46 (HONO), m/z 96, m/z 102 and m/z 113. None of these ions was observed to change during the experiments and they were monitored to ensure the CIMS was operating correctly. This list of ions was added to the text after line 12.

Section 2.1.2: What was the disodium phosphate concentration in your buffer? There is recent evidence that the solubility of organic molecules is modulated by salt concentration (e.g. Kampf et al. 2013, Endo et al. 2012, Wang et al. 2014, and Waxman et al. 2015). These effects are more pronounced at the higher salt concentrations typically found in aerosols. Is your phosphate concentration high enough to impact the solubility of HNCO?

The buffer solutions for the KH experiments were made with solid citric acid, disodium phosphate and deionized water with citric acid concentrations ranging from 0.02 M to 0.0035 M to access a pH range of 2.5-4.0 (page 24223, line 14). The buffer solutions for the hydrolysis experiments were all below 0.002 M. We believe that at these concentrations, the ionic strength of the solution is low enough to have minimal impact on the solubility of HNCO. However, the salting out effect for HNCO remains to be investigated.

Clarification was added to the text, which now reads, “All buffer concentrations were < 0.002 M, and we assume that the ionic strength of these solutions had minimal impact on the solubility of HNCO.”

Page 24223, lines 8-10: You state that the absolute gas phase concentration of HNCO is not required. This statement makes perfect sense once one has read the Results and Discussion section, but is confusing here as the reader will likely be assuming that you measure aqueous phase concentration and gas phase concentration to calculate M/atm. You could consider adding an additional sentence or two to elaborate on your analysis method to explain why this value is not necessary.

Good point. The sentence now reads, “the absolute concentration of gas-phase HNCO is not required in this approach since it relies on the decay of the signal, $[\text{HNCO}]_t/[\text{HNCO}]_0$ and not on the absolute gas phase and aqueous phase concentrations.”

Figures 3 and 4: Why show all measurements rather than average the measurements and propagate the error bars where you have multiple measurements?

Each point in these figures show a K_H^{eff} determined using 5 different flows at the same pH and same temperature. Each point cannot be averaged as they were determined at different pH and temperatures.

References cited:

Kampf, C. J.; Waxman, E. M.; Slowik, J. G.; Dommen, J.; Pfaffenberger, L.; Praplan, A. P.; Prevot, A. S. H.; Baltensperger, U.; Hoffmann, T.; Volkamer, R. Effective Henry's Law Partitioning and the Salting Constant of Glyoxal in Aerosols Containing Sulfate Environ. Sci. Technol. 2013, 47 (9) 4236– 4244, DOI: 10.1021/es400083d

Wang, C.; Lei, Y. D.; Endo, S.; Wania, F. Measuring and Modeling the Salting-out Effect in Ammonium Sulfate Solutions Environ. Sci. Technol. 2014, 48 (22) 13238– 13245, DOI: 10.1021/es5035602

Endo, S.; Pfennigsdorff, A.; Goss, K. U. Salting-Out Effect in Aqueous NaCl Solutions Increases with Size and Decreases with Polarities of Solute Molecule Environ. Sci. Technol. 2012, 46 (3) 1496– 1503, DOI: 10.1021/es203183z

Waxman, E. M.; Elm, J.; Kurten, T.; Mikkelsen, K. V.; Ziemann, P. J.; Volkamer, R. Glyoxal and Methylglyoxal Setschenow Salting Constants in Sulfate, Nitrate, and Chloride Solutions: Measurements and Gibbs Energies Environ. Sci. Technol. 2015, 49 (19), 11500–11508, DOI: 10.1021/acs.est.5b02782

Solubility and Reactivity of HNCO in Water: Insights into HNCO's Fate in the Atmosphere

N. Borduas¹, B. Place¹, G. R. Wentworth¹, J. P. D. Abbatt¹ and J. G. Murphy^{1,*}

[1]{Department of Chemistry, University of Toronto, Toronto, Ontario, Canada}

Correspondence to: J. G. Murphy (jmurphy@chem.utoronto.ca)

Abstract

A growing number of ambient measurements of isocyanic acid (HNCO) are being made, yet little is known about its fate in the atmosphere. To better understand HNCO's loss processes and particularly its atmospheric partitioning behavior, we measure its effective Henry's Law coefficient K_H^{eff} with a bubbler experiment using chemical ionization mass spectrometry as the gas phase analytical technique. By conducting experiments at different pH values and temperature, a Henry's Law coefficient K_H of $26 \pm 2 \text{ M atm}^{-1}$ is obtained, with an enthalpy of dissolution of $-34 \pm 2 \text{ kJ mol}^{-1}$, which translates to a K_H^{eff} of 31 M atm^{-1} at 298 K and at pH 3. Our approach also allows for the determination of HNCO's acid dissociation constant, which we determine to be $K_a = 2.1 \pm 0.2 \times 10^{-4} \text{ M}$ at 298 K. Furthermore, by using ion chromatography to analyze aqueous solution composition, we revisit the hydrolysis kinetics of HNCO at different pH and temperature conditions. Three pH dependent hydrolysis mechanisms are in play and we determine the Arrhenius expressions for each rate to be $k_1 = (4.4 \pm 0.2) \times 10^7 \exp(-6000 \pm 240 / T) \text{ M s}^{-1}$, $k_2 = (8.9 \pm 0.9) \times 10^6 \exp(-6770 \pm 450 / T) \text{ s}^{-1}$ and $k_3 = (7.2 \pm 1.5) \times 10^8 \exp(-10900 \pm 1400 / T) \text{ s}^{-1}$ where k_1 is for $\text{HNCO} + \text{H}^+ + \text{H}_2\text{O} \rightarrow \text{NH}_4^+ + \text{CO}_2$, k_2 is for $\text{HNCO} + \text{H}_2\text{O} \rightarrow \text{NH}_3 + \text{CO}_2$ and k_3 is for $\text{NCO}^- + 2 \text{ H}_2\text{O} \rightarrow \text{NH}_3 + \text{HCO}_3^-$. HNCO's lifetime against hydrolysis is therefore estimated to be 10 days to 28 years at pH values, liquid water contents, and temperatures relevant to tropospheric clouds, years in oceans and months in human blood. In all, a better parameterized Henry's Law coefficient and hydrolysis rates of HNCO allow for more accurate predictions of its concentration in the atmosphere and consequently help define exposure of this toxic molecule.

1 **1 Introduction**

2 Until recently, the interest in studying HNCO was from a fundamental science perspective with
3 research conducted on its structure, preparation and physical properties (Belson and Strachan
4 1982) and on its theoretical rovibrational spectra (Mladenović and Lewerenz 2008). Both
5 theoretical and experimental data indicate that HNCO is the most stable CHNO isomer with a
6 near-linear π -bond system (Hocking et al. 1975, Jones et al. 1950, Poppinger et al. 1977). In
7 2010, Roberts et al. reported detection of HNCO using negative ion proton transfer chemical
8 ionization mass spectrometry (CIMS) from laboratory biomass burning and later determined its
9 emission factor to be 0.25 – 1.20 mmol per mol of CO for different types of biomass fuels
10 (Veres et al. 2010). Shortly afterwards, the same authors reported the first ambient atmospheric
11 measurements of HNCO in Pasadena, California, reaching 120 pptv and raising concerns of
12 HNCO exposure due to its toxicity (Roberts et al. 2011). Indeed, HNCO has been observed to
13 cause protein carbamylation leading to cardiovascular disease, rheumatoid arthritis and
14 cataracts (Beswick and Harding 1984, Lee and Manning 1973, Mydel et al. 2010, Wang et al.
15 2007).

16 Since Roberts et al.'s initial measurements, ambient HNCO has also been measured in Boulder
17 and in Fort Collins, Colorado, (Roberts et al. 2014), in Toronto, Ontario (Wentzell et al. 2013)
18 and in Calgary, Alberta (Woodward-Massey et al. 2014). HNCO has also been detected
19 simultaneously in the gas phase and in cloud water in La Jolla, California (Zhao et al. 2014).
20 From these studies, typical urban concentrations range from below detection limits to
21 approximately 100 pptv, whereas concentrations as high as 1.2 ppbv, enough to be of health
22 concern, have been measured in air masses impacted by biomass burning in Boulder, Colorado
23 (Roberts et al. 2011, Roberts et al. 2014, Woodward-Massey et al. 2014).

24 HNCO has a variety of anthropogenic and biogenic sources to the atmosphere. HNCO has been
25 quantified from diesel engine exhaust (Kroeher et al. 2005, Wentzell et al. 2013) and light duty
26 vehicles (Brady et al. 2014) as well as from biogenic sources such as biomass burning (Roberts
27 et al. 2010, Roberts et al. 2011, Roberts et al. 2014, Veres et al. 2010). There also exist
28 secondary sources of HNCO to the atmosphere, including the gas phase oxidation of amines
29 and amides by OH radicals producing HNCO via H-abstraction mechanisms (Barnes et al.
30 2010, Borduas et al. 2013, Borduas et al. 2015). Evidence of secondary sources of HNCO has
31 also been demonstrated in the field, with peak HNCO concentrations occurring during daytime
32 (Roberts et al. 2011, Roberts et al. 2014, Zhao et al. 2014)

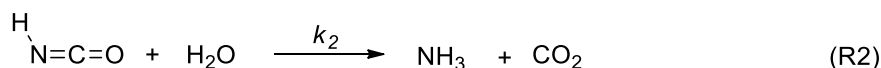
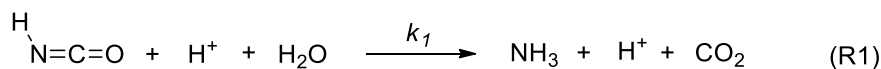
1 The sinks of HNCO however remain poorly constrained. HNCO has a lifetime of decades
2 towards OH radicals in the atmosphere as estimated by extrapolating high temperature rate
3 coefficients to atmospheric temperatures (Tsang 1992, Mertens et al. 1992, Tully et al. 1989).
4 It is also not expected to photolyze in the actinic region since its first UV absorption band is
5 observed below 280 nm wavelengths (Brownsword et al. 1996, Dixon and Kirby 1968, Rabalais
6 et al. 1969). Nonetheless, HNCO has served as a benchmark system in understanding
7 photodissociation decomposition pathways such as direct and indirect dissociation processes
8 and remains an area of active research (Yu et al. 2013) and references therein. HNCO is most
9 likely removed from the atmosphere by wet and/or dry deposition. HNCO's gas-to-liquid
10 partitioning is therefore an important thermodynamic property that can be used to predict its
11 atmospheric fate. Specifically, the Henry's Law coefficient K_H for the solubility of HNCO
12 represents the equilibrium ratio between its gas phase and aqueous phase concentrations at
13 infinite dilutions according to Eq. (1) (Sander 2015, Sander 1999). The Henry's Law coefficient
14 for HNCO has only recently been measured by Roberts and coworkers but their experimental
15 set up was limited to a single pH measurement (Roberts et al. 2011). As HNCO is a weak acid
16 with a pK_a of 3.7, its Henry's Law coefficient is expected to have a large pH dependence as
17 described in Eq. (2). Furthermore, the enthalpy of dissolution for HNCO is currently unknown.
18 In lieu of measurements, modelling studies on HNCO have used formic acid's enthalpy of
19 dissolution to model the temperature dependence of HNCO's Henry's Law coefficient (Barth
20 et al. 2013, Young et al. 2012). In our present study, we measure the effective Henry's Law
21 coefficient of HNCO at a range of pH and temperatures to determine its enthalpy of dissolution
22 for the first time.

23
$$K_H = C_{HNCO} / p_{HNCO} \quad (1)$$

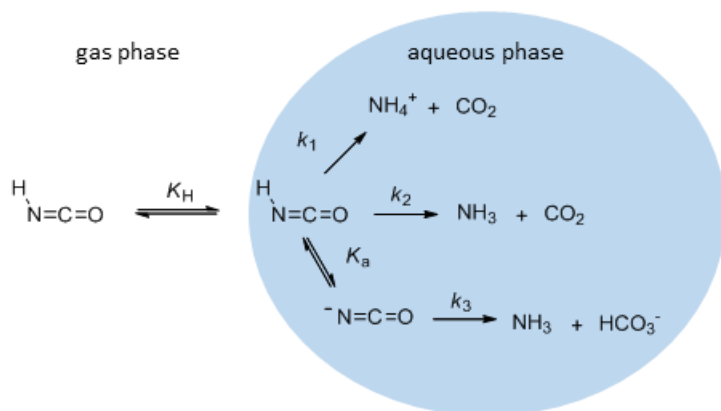
24
$$K_H^{\text{eff}} = K_H \left(1 + \frac{K_a}{[H^+]} \right) \quad (2)$$

25 HNCO reacts irreversibly with water in the aqueous phase, an unusual property for an
26 atmospheric molecule. Once HNCO partitions to the aqueous phase, three mechanisms for its
27 hydrolysis are possible. The first (R1) is acid-catalysed and is therefore termolecular whereas
28 the second (R2) and third (R3) are bimolecular reactions involving either the protonated or
29 deprotonated form of HNCO (Scheme 1) (Amell 1956, Belson and Strachan 1982, Jensen
30 1958). In 1958, Jensen determined the hydrolysis rate of the three mechanisms through addition
31 of $AgNO_3$ to buffered solutions at different time points to precipitate unreacted isocyanate as
32 $AgNCO$, followed by back titration of excess $AgNO_3$ with NH_4SCN . Considering the

1 importance of these mechanisms in evaluating the fate of HNCO in the atmosphere, we follow
 2 up on the study by Jensen with our own experiments using ion chromatography to determine
 3 the pH and temperature dependencies of the overall rate of hydrolysis of HNCO. Quantitative
 4 knowledge of the ability of HNCO to partition to the aqueous phase and its subsequent reactions
 5 with water allows for an accurate understanding of the chemical fate of HNCO in the
 6 atmosphere (Fig. 1). In this study, we therefore provide laboratory measurements of HNCO's
 7 Henry's Law coefficient and enthalpy of dissolution as well as its three rates of hydrolysis and
 8 their respective activation energies.



10 Scheme 1: The three mechanisms involved in HNCO's hydrolysis.



11
 12 Figure 1: The fate of HNCO in the atmosphere includes its partitioning between the gas and
 13 aqueous phases and its hydrolysis through three different mechanisms governed by k_1 , k_2 , and
 14 k_3 .

15 2 Experimental Methods

16 2.1 Henry's Law coefficient experiments

17 To measure the effective Henry's Law coefficient K_H^{eff} of HNCO, we use a bubbler column
 18 experimental set up and detect HNCO through chemical ionization mass spectrometry.

1 2.1.1 Acetate reagent ion CIMS

2 The quadrupole chemical ionization mass spectrometer (CIMS) was built in house and is
3 described in detail elsewhere (Escorcía et al. 2010). We opted to use acetate as the reagent ion
4 which has been shown to be sensitive for the detection of acids (Roberts et al. 2010, Veres et
5 al. 2008). For this experimental set up, the reagent ion was generated by flowing 20 sccm of
6 nitrogen over a glass tube containing acetic anhydride (from Sigma-Aldrich and used as is) and
7 maintained at 30 °C. This flow was subsequently mixed with a nitrogen dilution flow of 2 L
8 min⁻¹ and passed through a polonium-210 radioactive source to generate acetate ions. All flows
9 were controlled using mass flow controllers. The data acquisition was done under selected ion
10 mode where 10 m/z ratios were monitored with dwell times of 0.2 s each and each duty cycle
11 was 4 s. Ions measured included m/z 59 (AcO⁻), m/z 119 ((AcOH)AcO⁻), m/z 51 (black counts),
12 m/z 35 (Cl⁻), m/z 42 (NCO⁻), m/z 45 (HCOO⁻), m/z 46 (ONO⁻), m/z 96, m/z 102 and m/z 113.
13 The raw signals are then normalized to m/z 59 and reported as normalized counts per second
14 (ncps). For the exception of m/z 42, none of the ions were observed to change during the
15 experiments. The inlet flow of the CIMS ~~was is~~ governed by a pin hole at 0.5 L min⁻¹, governed
16 ~~by a pin hole,~~ and a N₂ dilution flow of 0.4 L min⁻¹ into the inlet was used to avoid depletion of
17 the acetate reagent ion by high HNCO concentrations. Previous work suggests there is no
18 significant role of water vapour in HNCO's detection by acetate CIMS (Roberts et al. 2010).
19 With the CIMS's inlet dilution, the RH within the ion molecule region was < 20%. The CIMS
20 monitors NCO⁻ at m/z 42. (Roberts et al. 2010)

21 2.1.2 Experimental set up for measurement of K_H

22 To obtain the Henry's Law coefficient, K_H , we monitored the decrease in gas phase HNCO
23 exiting a buffered aqueous solution for a range of volume flow rates ~~through the buffer.~~ Thus,
24 ~~a~~ A bubbler column experimental set up is used with online gas phase detection. This method is
25 employed to measure HNCO's partitioning and take into account the concurrent hydrolysis of
26 HNCO in the buffer solution at high time resolution. Our experimental setup is based on
27 previous work (Kames and Schurath 1995, Roberts 2005, Roberts et al. 2011) and our apparatus
28 is comprised of one fritted bubbler with an approximate volume of 70 mL which contained 15
29 mL of a citric acid/Na₂HPO₄ buffer at varying pH. The 15 mL volume was chosen to reduce
30 HNCO equilibration times and to simultaneously ensure that the bubbler's frit was submerged.
31 Experiments performed in 30 mL of buffer yielded identical results. The water lost to the gas
32 phase during the experiments (< 1 h) was at most 5% of the original buffer volume and so no

1 corrections to the latter were required. The bubbler was held in a temperature-controlled bath
2 of approximately 1:1 mixture of deionized water and ethylene glycol. Upstream of the bubbler,
3 where the RH was measured to be ~ 50%, was a valve and a tee connection where the dry
4 HNCO flow could be connected and disconnected during the experiments. Downstream of the
5 bubbler was another tee which connected to both the exhaust and the acetate reagent ion
6 ~~chemical ionization mass spectrometer (CIMS)~~ CIMS. Conveniently, the absolute concentration
7 of gas-phase HNCO is not required in this approach ~~since it relies on~~ since it relies on the decay
8 of the signal, $[\text{HNCO}]_t/[\text{HNCO}]_0$ and not on the absolute gas phase and aqueous phase
9 concentrations.

10 HNCO was produced using a permeation source which sublimes solid cyanuric acid at 250 °C
11 in a flow of dry nitrogen and is described in detail elsewhere-(Borduas et al. 2015). This source
12 is based on HNCO sublimation techniques and on a similar source previously developed by
13 Roberts et al. (Belson and Strachan 1982, Roberts et al. 2010). The buffer solutions were made
14 with solid citric acid, disodium phosphate and deionized water with citric acid concentrations
15 ranging from 0.02 M to 0.0035 M to access a pH range of 2.5-4.0.

16 Each experiment began with gaseous HNCO flowing through a fresh buffer solution until a
17 reasonably stable signal (> 0.01 ncps) was obtained by the CIMS (background counts $\sim 5 \times 10^4$
18 ncps). The solution did not need to reach equilibrium for the experiment to proceed and so
19 lower temperatures and higher pHs (when the equilibration time is longest and may reach over
20 4-5 hours) were feasible. Once a normalized signal (i.e. relative to the reagent ion signal) of at
21 least 0.025 for HNCO was obtained, the flow of HNCO through the bubbler was turned off,
22 and only pure nitrogen continued to flow through. The HNCO signal then decayed
23 exponentially as a function of time due to partitioning as well as hydrolysis. This decay was
24 monitored until it had decreased to less than one quarter of the original signal. This method also
25 has the advantage of extracting an effective Henry's Law coefficient without needing to monitor
26 the aqueous phase HNCO concentration.

27 **2.2 Hydrolysis rate experiments**

28 HNCO in the aqueous phase was measured using ion chromatography at different pH and
29 temperatures to determine its rates of hydrolysis.

1 2.2.1 Ion chromatography

2 The measurements for the hydrolysis of HNCO were made using a Dionex IC-2000 Ion
3 Chromatography (IC) System. An IonPac (AS19) anion column consisting of a quaternary
4 ammonium ion stationary phase with diameter and length dimensions of 4 mm and 25 mm
5 respectively was employed. Sample runs used a concentration gradient of the eluent KOH
6 ranging from 2 mM to 20 mM. An optimized elution program was written for each pH range
7 measured (between 25-60 minutes for each injection). Samples were injected using a Dionex
8 (AS40) automated sampler into a 25 μ L loop for pre-injection. The use of a loop rather than a
9 concentrator was important and ensured that the total HNCO/NCO⁻ concentrations were being
10 measured. The IC was calibrated using matrix-matched standards of known HNCO/NCO⁻
11 concentrations prepared from serial dilutions of KOCN (Sigma-Aldrich, 96% purity).

12 2.2.2 Hydrolysis kinetics experiments

13 The kinetics of the hydrolysis reactions in the pH range of 1-2 are very fast; complete decays
14 occurred in a matter of minutes. The decay of HNCO at these low pH values is therefore too
15 quick for the 25 min IC method to capture. To circumvent this issue, we used a quenching
16 method. Specifically, we prepared an aqueous solution of 50 mL of sulphuric acid at the desired
17 pH. 5 mL of this acidic solution was subsequently added to a 0.02 M solution of KOCN in eight
18 different falcon tubes to initiate the rapid hydrolysis reaction. Each reaction was then quenched
19 at different times by a 0.1 M aqueous solution of KOH. Increasing the pH to more than 10
20 slowed the hydrolysis kinetics by orders of magnitude and allowed for subsequent IC
21 measurements. Replacing sulphuric acid by nitric acid and/or KOH by NaOH yielded identical
22 hydrolysis rates and ensured the results were reproducible with different acids and bases.

23 Buffer solutions in the pH range of 3-5 were prepared by using appropriate molar ratios of citric
24 acid and disodium phosphate whereas buffer solutions in the pH range of 9-10 used sodium
25 carbonate and sodium bicarbonate. All buffer concentrations were < 0.002 M, and we assume
26 that the ionic strength of these solutions had minimal impact on the solubility of HNCO. For
27 the room temperature set of kinetic experiments, the experiment was initiated by the addition
28 of 0.1 g of KOCN to 50 mL of the desired buffer solution. The solution was further diluted by
29 a factor of 500 and then split into 8 samples for analysis at succeeding intervals on the anion
30 IC.

1 Hydrolysis reactions were run at different temperatures to assess the activation energies of each
 2 of the three hydrolysis mechanisms. Room temperature reactions were conducted inside the IC
 3 autosampler AS40 (with a cover) and monitored by a temperature button (iButtons, Maxim
 4 Integrated, San Jose, CA with 0.5 °C resolution)). Colder temperature reactions were done in a
 5 water ice bath and monitored by a thermometer. Finally, warmer temperature reactions for high
 6 pH samples were run in a temperature-controlled water bath. These reactions took days to
 7 weeks to reach completion, and so 5 mL samples from the reaction mixtures were taken out of
 8 the water bath and measured on the IC at appropriate time intervals.

9 **3 Results and Discussion**

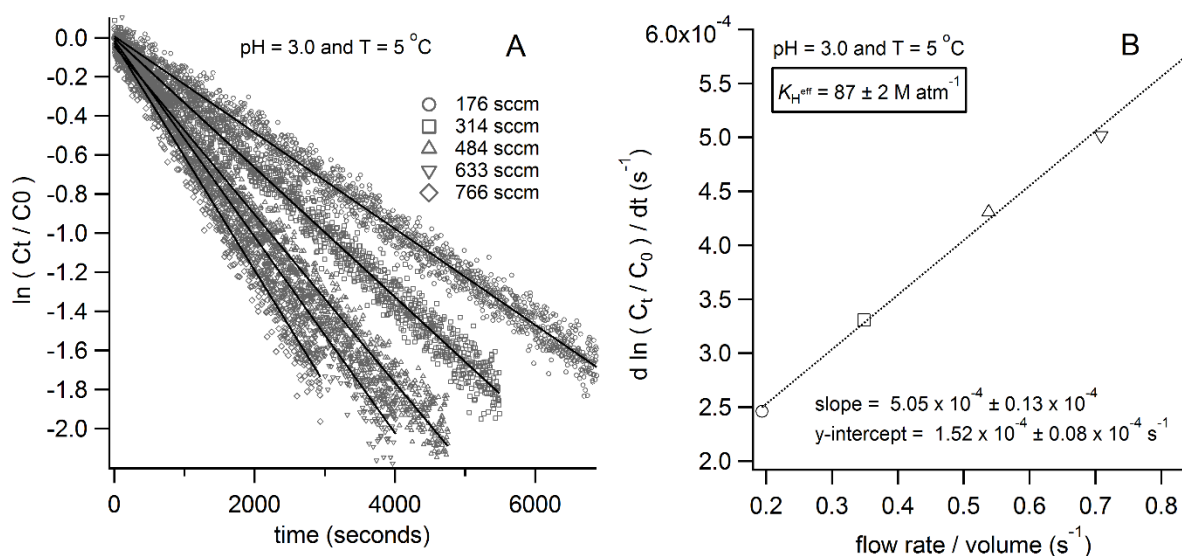
10 **3.1 Henry's Law coefficient K_H**

11 HNCO's effective Henry's Law solubility coefficient K_H^{eff} expressed in M atm^{-1} was determined
 12 based on the exponential decay of gaseous HNCO exiting a bubbler containing a buffered
 13 solution. The observed decay of HNCO is caused by its partitioning from the aqueous phase to
 14 the gas phase as well as its competing hydrolysis reaction. Equation (3) represents the rate law
 15 for the disappearance of HNCO during the experiment and Eq. (4) is the integrated rate law.

$$16 \quad -\frac{d[\text{HNCO}]}{dt} = [\text{HNCO}] \frac{\varphi}{K_H^{\text{eff}} V R T} + [\text{HNCO}] k_{\text{hyd}} \quad (3)$$

$$17 \quad \ln \frac{[\text{HNCO}]_t}{[\text{HNCO}]_0} = - \left[\frac{\varphi}{K_H^{\text{eff}} V R T} + k_{\text{hyd}} \right] t \quad (4)$$

18 Where $[\text{HNCO}]_t$ is the HNCO concentration at time t , $[\text{HNCO}]_0$ is the initial HNCO
 19 concentration (at time $t = 0$), $[\text{HNCO}]_t/[\text{HNCO}]_0$ is the HNCO concentration in the gas phase
 20 downstream of the bubbler measured by the CIMS, φ is the volumetric flow rate ($\text{cm}^3 \text{s}^{-1}$), K_H^{eff} is
 21 the effective Henry's Law coefficient for solubility ($\text{mol L}^{-1} \text{atm}^{-1}$), V is the liquid volume of the
 22 buffer (cm^3), R is the ideal gas constant ($8.21 \times 10^{-2} \text{ L atm mol}^{-1} \text{K}^{-1}$), T is the temperature (K),
 23 k_{hyd} is HNCO's overall rate of hydrolysis (s^{-1}) and t is the time (s). To extract the value of K_H^{eff}
 24 from the experimental decay curves, we first plot the natural logarithm of change in HNCO
 25 concentration versus time for different flow rates ranging from 175 to 800 sccm as shown in
 26 Fig. 2A. The slope of each experiment is then plotted as function of the ratio of the flow rate
 27 and volume depicted in Fig. 2B. The slope of Fig. 2B leads to a value representing $(K_H^{\text{eff}} R T)^{-1}$
 28 and so K_H^{eff} can be calculated.

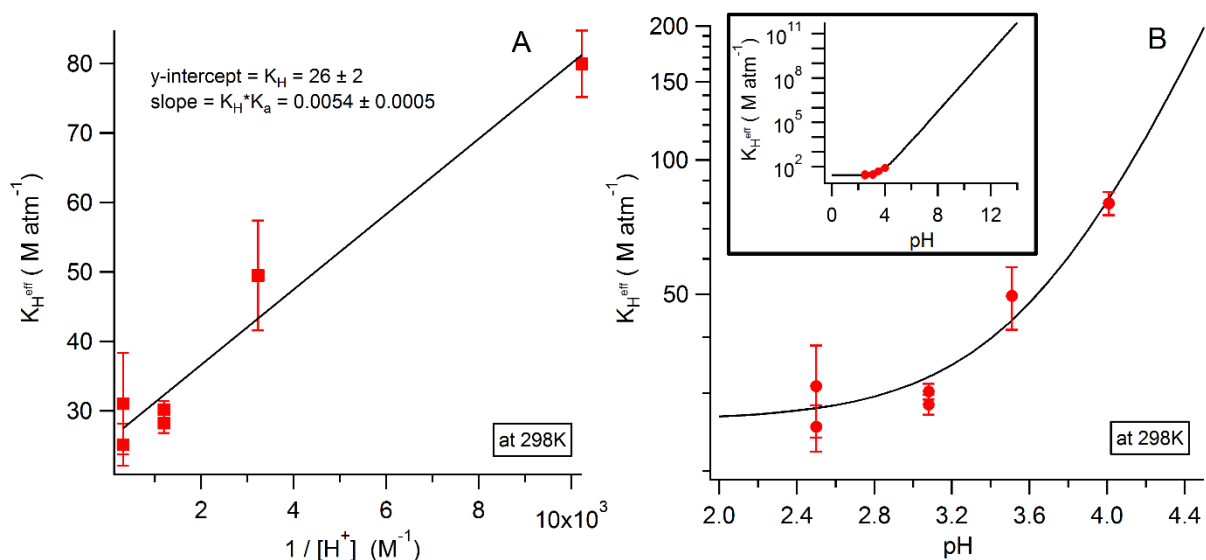


1
 2 Figure 2: A) The concentration decay curves as a function of time according to Eq. (4) for each
 3 flow rate shown; B) The slopes of each fit in Fig. 2A plotted as a function of the ratio of the
 4 flow rate to the volume. The symbols in both figures represent the same flow rate shown.

5 These dynamic experiments were repeated with a range of buffer solutions ranging from pH
 6 2.5-4.0 to determine the pH-independent Henry's Law coefficient, K_H , of H₂CO₃*. Experiments
 7 at temperatures of 273-298 K were also conducted to determine H₂CO₃*'s enthalpy of
 8 dissolution, ΔH_{diss} .

9 3.1.1 pH dependence of K_H^{eff}

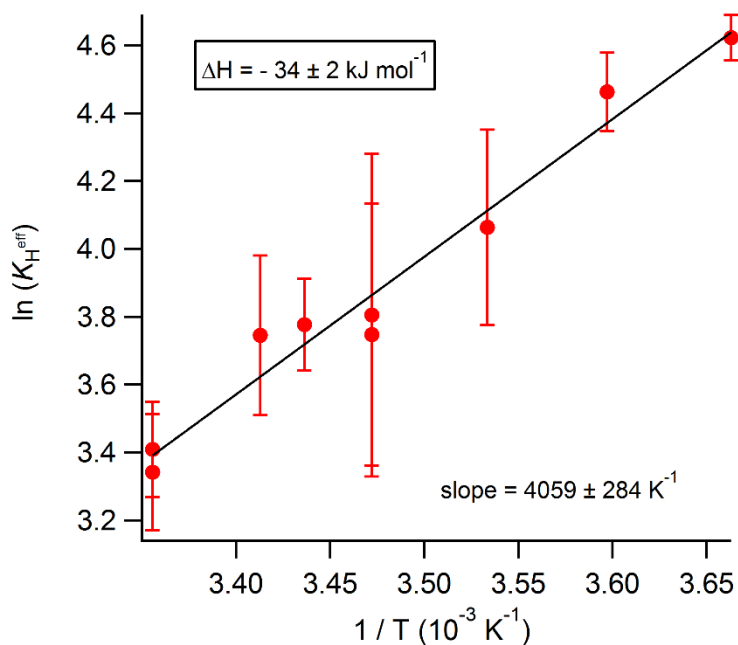
10 The pH dependence of the effective Henry's Law coefficient K_H^{eff} of a weak acid like H₂CO₃*
 11 depends on its pK_a as well as on the pH according to Eq. (2). Throughout our experiments, we
 12 measure the value of K_H^{eff} and employ Eq. (2) to plot K_H^{eff} as a function of the inverse of the
 13 proton concentration, [H⁺], and thus to extract H₂CO₃*'s Henry's Law coefficient for solubility,
 14 K_H . Figure 3A depicts this linear relationship and yields a value of $26 \pm 2 \text{ M atm}^{-1}$ for K_H . Our
 15 K_H value compares well with the only other published value of 21 M atm^{-1} determined solely at
 16 pH 3 (Roberts et al. 2011). Figure 3B on the other hand shows experimentally determined K_H^{eff}
 17 at different pH values and at a constant temperature of $298.0 \pm 0.2 \text{ K}$. Error bars in both Fig.
 18 3A and 3B represent the percentage of the standard deviation of the slope as in Fig. 2B. The
 19 slope in Fig. 3A also allows us to determine H₂CO₃*'s acid dissociation constant, K_a , which at
 20 298 K is $2.1 \pm 0.2 \times 10^{-4} \text{ M}$. Our K_a value also agrees well with previously reported K_a for
 21 H₂CO₃* (Amell 1956, Belson and Strachan 1982).



1
 2 Figure 3: A) The fit according to Eq. (2) of the experimental K_H^{eff} values which allows for the
 3 determination of K_H and K_a at 298 K. B) The experimental K_H^{eff} values as a function of pH at
 4 298 K. The black line is the modelled dependence of K_H^{eff} according to Eq. (2) based on the
 5 determined value of K_H and a value for K_a of 2.1×10^{-4} M. The inset shows the range of K_H^{eff}
 6 across the full range of pH.

7 3.1.2 Temperature dependence

8 The temperature dependence of HNCO's solubility was established by running experiments at
 9 varying temperatures from 273 to 298 K. Since K_H^{eff} is very sensitive to pH changes, all
 10 experiments were conducted with a buffer solution from the same batch and same volumetric
 11 flask within a few days. Plotting the natural logarithm of the effective Henry's Law coefficient
 12 as a function of the inverse of temperature yields the ratio of the enthalpy of dissolution, ΔH_{diss} ,
 13 to the gas constant, R (Fig. 4). We report a value of -34 ± 2 kJ mol⁻¹ for HNCO's enthalpy of
 14 dissolution, where the uncertainty stems from the deviation from the slope depicted in Figure
 15 4. This value compares to similar weak acids like HONO (-40 kJ mol⁻¹) and HCN (-42 kJ
 16 mol⁻¹), but differs from the value of formic acid (-47 kJ mol⁻¹) which was the value assumed
 17 for HNCO in the Young et al. and the Barth et al. modelling studies (Barth et al. 2013, Sander
 18 2015, Young et al. 2012).



1
2 Figure 4: The temperature dependence of experimentally measured K_H^{eff} at pH 3.08.

3 3.2 Rate of hydrolysis k_{hyd}

4 There are three mechanisms by which HNCO can react with water described in Scheme 1 (R1)
5 to (R3) and depicted in Fig. 1. The disappearance of HNCO in the aqueous phase can therefore
6 be described by the rate law shown as Eq. (5). The pH dependence of HNCO's hydrolysis
7 manifests itself in the first term of Eq. (5) as the hydrogen ion concentration as well as in the
8 concentration of the dissociated/non-dissociated acid in each term.

$$9 \quad -\frac{d[\text{HNCO}]_t}{dt} = k_1[\text{HNCO}][\text{H}^+] + k_2[\text{HNCO}] + k_3[\text{NCO}^-] \quad (5)$$

10 To mathematically integrate this rate law, the concentration of HNCO needs to be expressed as
11 the sum of undissociated HNCO and of isocyanate ion NCO^- in solution, which is denoted in
12 Eq. (6) as $[\text{HNCO}]_{\text{tot}}$. HNCO's acid dissociation constant K_a relates the concentration of HNCO
13 and NCO^- as shown in Eq. (6). The K_a -dependant expression of Eq. (6) is then substituted into
14 the rate law of Eq. (5), and subsequently integrated. The K_a value of HNCO has a slight
15 temperature dependence with a heat of dissociation previously measured to be 5.4 kJ mol^{-1} ,
16 which for the temperature range of 273 to 298 K represents a 25% change (Amell 1956). We
17 therefore use Amell's heat of dissociation value throughout our analysis to account for K_a 's
18 temperature dependence in the van't Hoff equation. Furthermore, Belson et al.'s evaluation of
19 the K_a of HNCO literature recommends $2.0 \times 10^{-4} \text{ M}$ at 298 K (Belson and Strachan 1982).

1 Finally, our own work on the pH dependence of Henry's Law coefficient of HNCO, suggests a
 2 K_a value of $2.1 \pm 0.2 \times 10^{-4}$ M at 298 K, consistent with the recommended value (Fig. 3A).

$$3 \quad [HNCO] = [HNCO]_{tot} - [NCO^-] = \frac{[H^+][NCO^-]}{K_a} = \frac{[HNCO]_{tot}[H^+]}{K_a + [H^+]} \quad (6)$$

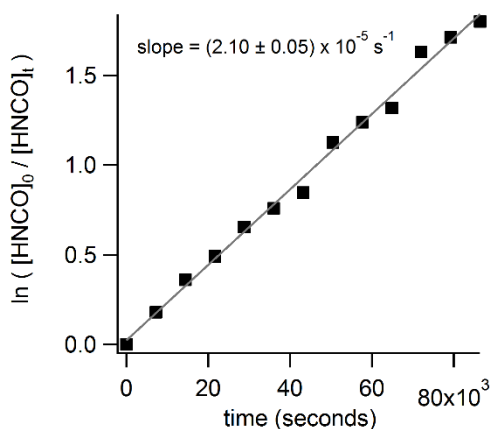
4 By integrating Eq. (5) with the appropriate substitutions, the resulting expression is Eq. (7),
 5 where k_{hyd} represents the observed first-order rate loss of hydrolysis of HNCO and depends on
 6 the individual reaction rates k_1 , k_2 and k_3 according to Eq. (8).

$$7 \quad \frac{[HNCO]_t}{[HNCO]_0} = e^{-k_{hyd}t} \quad (7)$$

$$8 \quad k_{hyd} = \frac{k_1[H^+]^2 + k_2[H^+] + k_3K_a}{K_a + [H^+]} \quad (8)$$

9 The aim of our hydrolysis experiments is to measure k_{hyd} at different pH values to subsequently
 10 solve for the values of the individual hydrolysis rate coefficients k_1 , k_2 and k_3 . To measure k_{hyd} ,
 11 we employ ion chromatography (IC) which allows for quantitative measurement of the total
 12 isocyanic acid in solution as NCO^- using an anion chromatography column. The key to making
 13 $[HNCO]_{tot}$ measurements was to use a loop injection port for the IC instead of a concentrator
 14 column, since the latter retains only ions and would not measure any protonated HNCO in
 15 solution. Appropriate buffer solutions were made to conduct experiments over a range of pH
 16 values from 1.7 to 10.4. The decay of $[HNCO]_{tot}$ was monitored by IC over time and plotting
 17 the natural logarithm of the decay as a function of time as in Fig. 5 yields the k_{hyd} specific to
 18 that temperature and pH. Hydrolysis experiments are listed in Table A1 in Appendix A.

19



20

21 Figure 5: Example of a hydrolysis experiment at pH 5.4 and at 25 °C where the $[HNCO]_{tot}$ is
 22 measured by loop injections on the IC.

1 3.2.1 Determining k_1 and k_2

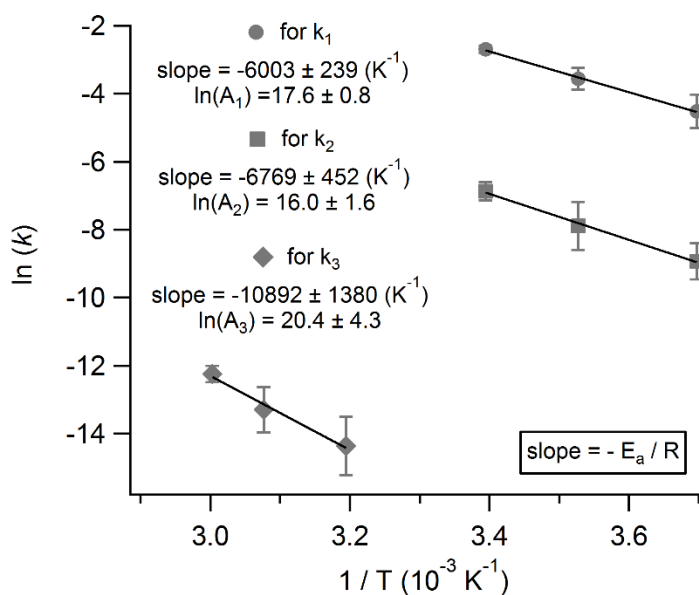
2 At a pH below 3, the third hydrolysis mechanism (Scheme 1 (R3)) will contribute minimally to
3 the overall k_{hyd} . Indeed, the third term in Eq. (8), $k_3K_a/(K_a+[H^+])$ will become very small because
4 $[H^+] \gg K_a$. Furthermore, very little of the HNCO is present as NCO^- at low pH. This
5 assumption (which we verify retroactively) simplifies the k_{hyd} expression to Eq. (9) with only
6 two unknowns, k_1 and k_2 . We can now solve for k_1 and k_2 from two k_{hyd} values derived from
7 experiments conducted at two different pH values but at the same temperature. For example,
8 solving for k_1 and k_2 at 295 K using the k_{hyd} in Table A1, we obtain a value of $(6.73 \pm 0.27) \times$
9 10^{-2} M s^{-1} for k_1 and of $(1.04 \pm 0.04) \times 10^{-3} \text{ s}^{-1}$ for k_2 . We do this calculation once per
10 temperature. The uncertainties associated with these measurements come from the slope of
11 decay of aqueous phase HNCO measured by IC.

$$12 \quad k_{hyd@pH<2.7} = \frac{k_1[H^+]^2 + k_2[H^+]}{K_a + [H^+]} \quad (9)$$

13 3.2.2 Temperature dependence of k_1 and k_2

14 Hydrolysis experiments of HNCO at three different temperatures further enables us to solve for
15 the temperature dependence of k_1 and k_2 . We chose three temperatures relevant to tropospheric
16 air masses: 270, 283 and 295 K. Figure 6 represents the slope of the natural logarithm of the
17 rate coefficient of hydrolysis as a function of the inverse of the temperature which according to
18 the Arrhenius equation shown in Eq. (10) yields the activation energy specific to each
19 hydrolysis mechanism. We obtain activation energies of $50 \pm 2 \text{ kJ mol}^{-1}$ and $56 \pm 4 \text{ kJ mol}^{-1}$ for
20 k_1 and k_2 respectively. Furthermore, the y-intercept of these linear plots yields the value of $\ln(A)$
21 in Eq. (10) and so the A factors of each hydrolysis mechanism can also be obtained, providing
22 Arrhenius expressions of $k_1 = (4.4 \pm 0.2) \times 10^7 \exp(-6000 \pm 240 / T) \text{ M s}^{-1}$ and $k_2 = (8.9 \pm 0.9)$
23 $\times 10^6 \exp(-6770 \pm 450 / T) \text{ s}^{-1}$. The uncertainties stem from the fit to the data points in Figure 6
24 (and their error bars comes from the slope of the decay of aqueous phase HNCO measured by
25 IC).

$$26 \quad k = Ae^{-E_a/RT} \quad (10)$$



1
2 Figure 6: The linear plots of the natural logarithm of each hydrolysis rate coefficient k_1 , k_2 and
3 k_3 as a function of the inverse of temperature to yield the activation energies of each mechanism.

4 3.2.3 Determining k_3 and its temperature dependence

5 At high pH levels, the third hydrolysis mechanism (Scheme 1 (R3)) will dominate the observed
6 k_{hyd} , however, the first two mechanisms may still have a non-negligible contribution to k_{hyd} and
7 can therefore not be disregarded. We can solve for k_3 , knowing k_1 and k_2 and their respective
8 temperature dependencies, using Eq. (8). The k_{hyd} values measured at pH above 9 and at 40 °C
9 are used (Table A1), and k_3 is determined for each pH. The average of our three measurements
10 at 40 °C is $(5.77 \pm 0.35) \times 10^{-7} \text{ s}^{-1}$. The temperature dependence of k_3 is determined in an
11 analogous way to k_1 and k_2 and is also depicted in Fig. 6. We obtain a value of $91 \pm 12 \text{ kJ mol}^{-1}$
12 which translates to an Arrhenius expression of $k_3 = (7.2 \pm 1.5) \times 10^8 \exp(-10900 \pm 1400 / T)$
13 s^{-1} .

14 Equipped with the values of k_1 , k_2 and k_3 and their temperature dependencies, a map of the
15 expected total hydrolysis rate, k_{hyd} , as a function of temperature and pH can be generated using
16 Eq. (8) and Eq. (10) and is plotted as Fig. 7. For reference, the colour scale of Fig. 7 also reads
17 in hydrolysis lifetime of HNCO in hours. It is clear that HNCO's lifetime in the aqueous phase
18 has a large temperature and pH dependence.

3.2.4 Comparing the rate of hydrolysis k_{hyd} through different methods

The individual rate coefficients of the three hydrolysis mechanisms (Scheme 1 (R1) to (R3)) have only been evaluated one other time in the literature (Jensen 1958). Our IC experimental method differs substantially from Jensen's back titration method, and yet we obtain similar values for k_1 , k_2 and k_3 as well as for their respective activation energies. The values are summarized in Table 2. Again, the colour scale of Fig. 7 is generated from Eq. (8) using our obtained values for k_1 , k_2 and k_3 and for E_{a1} , E_{a2} and E_{a3} , and we superimpose all our k_{hyd} measurements from Table A1 as circles. We further add Jensen's published raw data for comparison (Jensen 1958) as triangles. The agreement is good and is consistently within the same order of magnitude (Fig. 7).

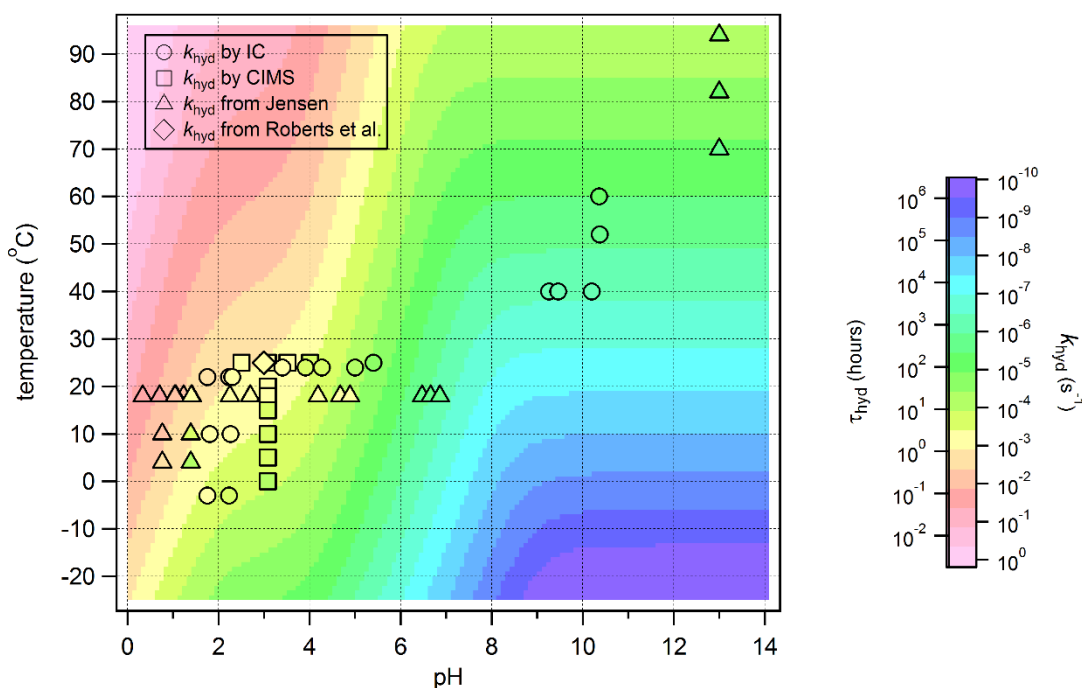
Table 2: HNCO's Henry's Law coefficient, acid dissociation constant and hydrolysis constants

Physical parameter	Value	Energy	Reference
Henry's Law coefficient, K_H	$26 \pm 2 \text{ M atm}^{-1}$	$\Delta H_{diss} = -34 \pm 2 \text{ kJ mol}^{-1}$	This work
	21 M atm^{-1}	–	Roberts et al. 2011
Acid dissociation constant, K_a^*	$2.1 \pm 0.2 \times 10^{-4} \text{ M}$	–	This work
	$2.0 \times 10^{-4} \text{ M}$	$\Delta H_{diss} = -5.4 \text{ kJ mol}^{-1}$	Amell 1956
Hydrolysis rate coefficient, k_1^*	$7.6 \pm 0.3 \times 10^{-2} \text{ s}^{-1}$	$E_{a1} = +50 \pm 2 \text{ kJ mol}^{-1}$	This work
	$1.1 \times 10^{-1} \text{ s}^{-1}$	$E_{a1} = +63 \text{ kJ mol}^{-1}$	Jensen 1958
Hydrolysis rate coefficient, k_2^*	$1.4 \pm 0.1 \times 10^{-3} \text{ s}^{-1}$	$E_{a2} = +56 \pm 4 \text{ kJ mol}^{-1}$	This work
	$1.8 \times 10^{-3} \text{ s}^{-1}$	$E_{a2} = +83 \text{ kJ mol}^{-1}$	Jensen 1958
Hydrolysis rate coefficient, k_3^*	$8.1 \pm 1.7 \times 10^{-8} \text{ s}^{-1}$	$E_{a3} = +91 \pm 12 \text{ kJ mol}^{-1}$	This work
	$1.2 \times 10^{-8} \text{ s}^{-1}$	$E_{a3} = +100 \text{ kJ mol}^{-1}$	Jensen 1958

* at 298 K

In addition, our Henry's Law coefficient experiment provides a complimentary way to determine k_{hyd} at different temperatures and pH values. Indeed, the intercept of the line which fit the data of $\ln(C_i/C_0)/dt$ versus ϕ/V yields k_{hyd} , representing the value for the loss process in the solution of the bubbler column experiment (an example is given in Fig. 2B). We show these values as squares in Fig. 7. Roberts et al. also determined k_{hyd} through this method at pH 3 and

1 at 25 °C and this value is appended to Fig. 7 (Roberts et al. 2011) as a diamond. The agreement
 2 is good from all four cases. We can conclude that the lifetime of HNCO against hydrolysis in
 3 dilute aqueous solutions spans seconds to years depending on pH and temperature. The lifetime
 4 of HNCO against hydrolysis in cloud water of pH 3-6 will be shorter and range from 10 hours
 5 to ~20 days in the troposphere. On the other hand, HNCO's hydrolysis in ocean waters of pH
 6 ~8.1 and temperatures below 30 °C will be very slow, translating to a lifetime of 1-2 years if
 7 we assume no other reactive chemistry is taking place. Finally, in the context of exposure, if
 8 HNCO is present in human blood at physiological pH and temperature, its lifetime to hydrolysis
 9 will be as high as several months. On the other hand, if HNCO is present in the stomach, which
 10 is more acidic, we would expect its lifetime to drop to minutes or hours.



11
 12 Figure 7: k_{hyd} as function of temperature and pH generated from Eq. (8) using our obtained
 13 values for k_1 , k_2 and k_3 and for E_{a1} , E_{a2} and E_{a3} . All available k_{hyd} measurements for HNCO in
 14 the literature and from this work are superimposed and colour coded appropriately. As a guide,
 15 the colour scale also represents the lifetime in hours for HNCO in dilute aqueous solutions.

16 4 Atmospheric Implications

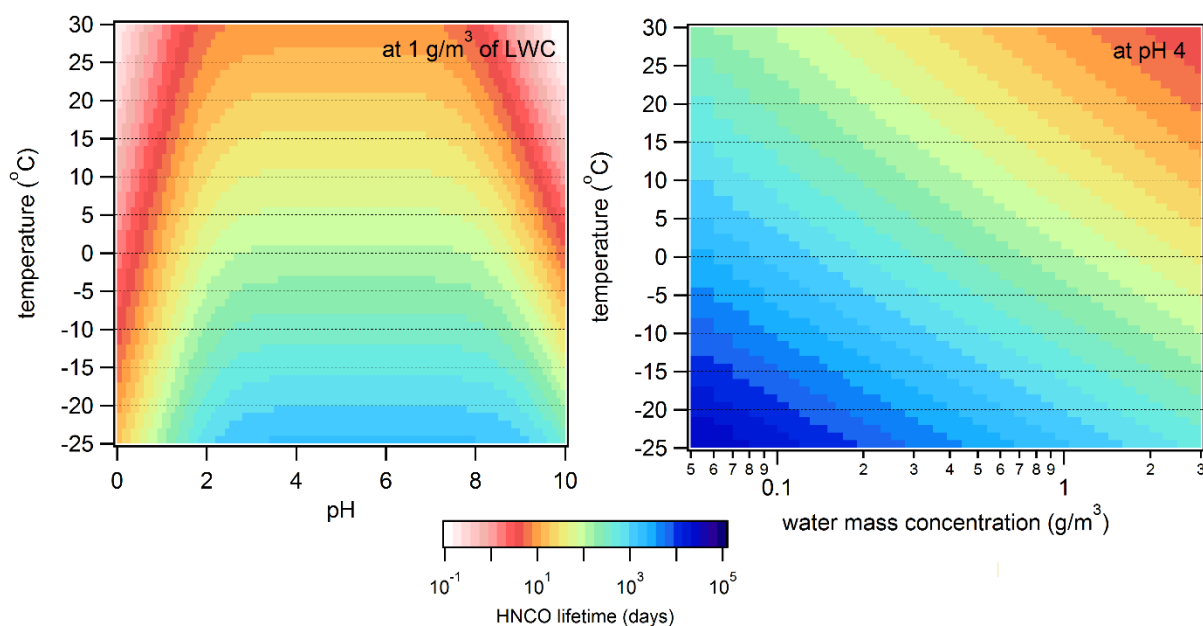
17 HNCO is a toxic molecule and can cause cardiovascular and cataract problems through protein
 18 carbamylation (Beswick and Harding 1984, Mydel et al. 2010, Wang et al. 2007). Recently
 19 reported ambient measurements of HNCO in North America raise concerns of exposure
 20 particularly from biomass burning, diesel and gasoline exhaust and urban environments (Brady

1 et al. 2014, Roberts et al. 2011, Roberts et al. 2014, Wentzell et al. 2013, Woodward-Massey
2 et al. 2014, Zhao et al. 2014). With the values for HNCO's Henry's Law coefficient and
3 hydrolysis rates reported here, a better understanding of HNCO's removal rate from the
4 atmosphere can be determined, and hence HNCO's atmospheric lifetime can be estimated. Note
5 however that our HNCO lifetime estimates do not consider dry deposition and therefore
6 represent a higher limit, particularly since Young et al. found that dry deposition can be
7 significant for HNCO (Young et al. 2012).

8 Specifically, the lifetime of HNCO in the atmosphere will depend on its partitioning to the
9 aqueous phase K_H^{eff} , the temperature T , the pH and liquid water content (LWC) of the
10 aerosol/droplet and finally the hydrolysis of HNCO k_{hyd} once in solution. We can calculate
11 HNCO's lifetime against hydrolysis based on Eq. (11) where τ is the lifetime in seconds, L is
12 the fraction of air volume occupied by liquid water (dimensionless) and R is the gas constant.
13 Figures 8A and 8B depict outputs of Eq. (11) with different fixed variables. Figure 8A holds
14 the LWC to 1 g m^{-3} , a value representative of cloud water, highlighting the dependence of
15 HNCO's lifetime on temperature and pH (Ip et al. 2009). At atmospherically relevant pH of 2
16 to 6 and at temperatures below $30 \text{ }^\circ\text{C}$, HNCO has a lifetime on the order of 10 days to hundreds
17 of years. Alternatively, Fig. 8B holds the pH at 4 and varies the LWC on the x-axis. Water
18 concentrations relevant to wet aerosol ($1\text{-}100 \text{ } \mu\text{g m}^{-3}$) are too small to act as a significant sink
19 for gas phase HNCO. However, Fig. 8B highlights the strong dependence of HNCO lifetime
20 on LWC in clouds, again ranging from days to hundreds of years. It therefore appears that if
21 HNCO is incorporated into cloud water, it is more likely to be rained out or revolatilized than
22 to hydrolyse given typical times in clouds of minutes to hours. There is also the possibility that
23 HNCO has other currently unknown sinks in cloud water that may be competitive with its
24 hydrolysis and further work on HNCO's aqueous phase chemistry with nucleophiles such as
25 amines and alcohols is ~~certainly warranted~~ currently underway in our laboratories. Finally,
26 HNCO will partition readily in oceans at pH ~ 8 , but will take years to hydrolyze.

27

$$\tau = 1/K_H^{\text{eff}} R T L k_{\text{hyd}} \quad (11)$$



1
 2 Figure 8: A) The lifetime of HNCO in days as a function of temperature and pH at 1 g m⁻³ of
 3 LWC and B) the lifetime of HNCO in days as a function of temperature and LWC at pH 4
 4 Zhao et al. (2014) observed higher concentrations of HNCO in the cloud water in La Jolla,
 5 California than predicted by its Henry's Law coefficient at 298 K(Zhao et al. 2014)(Zhao et al.
 6 2014)(Zhao et al. 2014). This observation remains puzzling but may point towards sources of
 7 HNCO within cloud water other than simple partitioning chemistry. The Barth et al. 2013
 8 modeling study concluded that fog, low-level stratus clouds or stratocumulus clouds were the
 9 most efficient cloud conditions at removing HNCO from the gas phase, particularly in polluted
 10 scenarios where the cloud water was more acidic. The authors highlighted the high dependence
 11 of HNCO's fate on liquid water pH and temperature, consistent with our findings (Barth et al.
 12 2013). The Young et al. 2012 study, which modelled global HNCO budgets, assumed the
 13 aqueous loss of the weak acid occurred only when the cloud liquid water content was greater
 14 than 1 mg m⁻³. Based on Fig. 8B, 1 mg m⁻³ is low for HNCO to significantly partition into the
 15 aqueous phase and rather requires water mass concentrations 1000 times greater for HNCO's
 16 lifetime to drop to days. The model may have overestimated the ability for LWC to act as a sink
 17 for HNCO. HNCO may be a longer lived species than previously thought and exposure of this
 18 toxic molecule may pose a threat to regions with HNCO point sources like biomass burning
 19 and engine exhaust, as pointed out by Young et al. in 2012 and Barth et al. in 2013.

1 5 Conclusions

2 In summary, we provide laboratory measurements of HNCO's important thermochemical
3 properties related to its behavior in water. We measured its Henry's Law coefficient using a
4 bubbler column experiment to be $26 \pm 2 \text{ M atm}^{-1}$ with an enthalpy of dissolution of $-34 \pm 2 \text{ kJ}$
5 mol^{-1} . Using ion chromatography, we determined the Arrhenius expression of HNCO's three
6 hydrolysis mechanisms: $k_1 = (4.4 \pm 0.2) \times 10^7 \exp(-6000 \pm 240 / T) \text{ M s}^{-1}$, $k_2 = (8.9 \pm 0.9) \times 10^6$
7 $\exp(-6770 \pm 450 / T) \text{ s}^{-1}$ and $k_3 = (7.2 \pm 1.5) \times 10^8 \exp(-10900 \pm 1400 / T) \text{ s}^{-1}$. These values will
8 provide better constraints on the sinks and thus lifetime of HNCO in the atmosphere with the
9 aim of minimizing exposure of this toxic molecule.

10 Appendix A:

11 Table A1: Compilation of k_{hyd} experiments at different pH and temperatures

pH	T (K)	$k_{hyd} (\text{S}^{-1})$
1.75	270	$(8.30 \pm 0.64) \times 10^{-4}$
1.75	295	$(2.22 \pm 0.06) \times 10^{-3}$
1.81	283	$(1.17 \pm 0.06) \times 10^{-3}$
2.23	270	$(1.92 \pm 0.16) \times 10^{-4}$
2.23	295	$(1.39 \pm 0.02) \times 10^{-3}$
2.26	283	$(5.13 \pm 0.28) \times 10^{-4}$
2.30	295	$(1.09 \pm 0.04) \times 10^{-3}$
3.40	297	$(9.90 \pm 0.25) \times 10^{-4}$
3.91	296	$(3.74 \pm 0.03) \times 10^{-4}$
4.27	296	$(2.99 \pm 0.02) \times 10^{-4}$
5.00	296	$(6.55 \pm 0.21) \times 10^{-5}$
5.40	298	$(2.10 \pm 0.05) \times 10^{-5}$
9.26	313	$(5.39 \pm 0.26) \times 10^{-7}$
9.46	313	$(6.07 \pm 0.28) \times 10^{-7}$
10.20	313	$(6.03 \pm 0.33) \times 10^{-7}$
10.36	333	$(4.84 \pm 0.09) \times 10^{-6}$
10.37	325	$(1.70 \pm 0.09) \times 10^{-6}$

1 **Author contribution**

2 N.B. designed the experimental approach with critical input from J. P. D. A. and J. G. M. on
3 the mass spectrometry method and from J. G. M. and G. R. W. on the ion chromatography
4 method. N. B. undertook the Henry's Law experiments and B. P. conducted the HNCO
5 hydrolysis experiments. N. B. analysed the data from both sets of experiments and N. B. wrote
6 the manuscript with feedback from all co-authors.

7 **Acknowledgements**

8 The authors acknowledge Erin Evoy for early work on the IC. N.B. acknowledges funding from
9 the University of Toronto Adel Sedra Graduate Fellowship. Operational support has been
10 provided by a grant from Environment Canada. The authors also acknowledge funding from
11 CFI and NSERC Discovery.

12 **References**

- 13 Amell, A. R.: Kinetics of the hydrolysis of cyanic acid, *J. Am. Chem. Soc.*, 78, 6234-6238,
14 1956.
- 15 Barnes, I., Solignac, G., Mellouki, A. and Becker, K. H.: Aspects of the atmospheric
16 chemistry of amides, *ChemPhysChem*, 11, 3844-3857, 2010.
- 17 Belson, D. J. and Strachan, A. N.: Preparation and properties of isocyanic acid, *Chem. Soc.*
18 *Rev.*, 11, 41-56, 1982.
- 19 Beswick, H. T. and Harding, J. J.: Conformational changes induced in bovine lens α -crystallin
20 by carbamylation, *Biochem. J.*, 223, 221-227, 1984.
- 21 Borduas, N., Abbatt, J. P. D. and Murphy, J. G.: Gas phase oxidation of monoethanolamine
22 (MEA) with OH radical and ozone: kinetics, products, and particles, *Environ. Sci. Technol.*,
23 47, 6377-6383, 2013.
- 24 Borduas, N., da Silva, G., Murphy, J. G. and Abbatt, J. P. D.: Experimental and theoretical
25 understanding of the gas phase oxidation of atmospheric amides with OH radicals: kinetics,
26 products, and mechanisms, *J. Phys. Chem. A*, 119, 4298-4308, 2015.
- 27 Brady, J. M., Crisp, T. A., Collier, S., Kuwayama, T., Forestieri, S. D., Perraud, V., Zhang,
28 Q., Kleeman, M. J., Cappa, C. D. and Bertram, T. H.: Real-time emission factor
29 measurements of isocyanic acid from light duty gasoline vehicles, *Environ. Sci. Technol.*, 48,
30 11405-11412, 2014.
- 31 Brownsword, R. A., Laurent, T., Vatsa, R. K., Volpp, H. - and Wolfrum, J.:
32 Photodissociation dynamics of HNCO at 248 nm, *Chem. Phys. Lett.*, 258, 164-170, 1996.

- 1 Dixon, R. N. and Kirby, G. H.: Ultra-violet absorption spectrum of isocyanic acid, Trans.
2 Faraday Soc., 64, 2002-2012, 1968.
- 3 Escorcia, E. N., Sjostedt, S. J. and Abbatt, J. P. D.: Kinetics of N₂O₅ hydrolysis on secondary
4 organic aerosol and mixed ammonium bisulfate secondary organic aerosol particles, J. Phys.
5 Chem. A, 114, 13113-13121, 2010.
- 6 Hocking, W. H., Gerry, M. C. L. and Winnewisser, G.: The Microwave and Millimetre Wave
7 Spectrum, Molecular Constants, Dipole Moment, and Structure of Isocyanic Acid, HNCO,
8 Can. J. Phys., 53, 1869-1901, 1975.
- 9 Ip, H. S. S., Huang, X. H. H. and Yu, J. Z.: Effective Henry's law constants of glyoxal,
10 glyoxylic acid, and glycolic acid, Geophys. Res. Lett., 36, L01802, 2009.
- 11 Jensen, M., B.: On the kinetics of the decomposition of cyanic acid, Acta Chem. Scand., 12,
12 1657-1670, 1958.
- 13 Jones, L. H., Shoolery, J. N., Shulman, R. G. and Yost, D. M.: The molecular structure of
14 isocyanic acid from microwave and infra- red absorption spectra, J. Chem. Phys., 18, 990-
15 991, <http://dx.doi.org/10.1063/1.1747827>, 1950.
- 16 Kames, J. and Schurath, U.: Henry's law and hydrolysis-rate constants for peroxyacyl nitrates
17 (PANs) using a homogeneous gas-phase source, J. Atmos. Chem., 21, 151-164, 1995.
- 18 Kroeher, O., Elsener, M. and Koebel, M.: An ammonia and isocyanic acid measuring
19 method for soot containing exhaust gases, Anal. Chim. Acta, 537, 393-400, 2005.
- 20 Lee, C. K. and Manning, J. M.: Kinetics of the carbamylation of the amino groups of sickle
21 cell hemoglobin by cyanate, J. Biol. Chem., 248, 5861-5865, 1973.
- 22 Mertens, J. D., Chang, A. Y., Hanson, R. K. and Bowman, C. T.: A shock tube study of
23 reactions of atomic oxygen with isocyanic acid, Int. J. Chem. Kinet., 24, 279-295, 1992.
- 24 Mladenović, M. and Lewerenz, M.: Equilibrium structure and energetics of CHNO isomers:
25 steps towards ab initio rovibrational spectra of quasi-linear molecules, Chem. Phys., 343, 129-
26 140, 2008.
- 27 Mydel, P., Wang, Z., Brisslert, M., Hellvard, A., Dahlberg, L. E., Hazen, S. L. and Bokarewa,
28 M.: Carbamylation-dependent activation of T cells: A novel mechanism in the pathogenesis
29 of autoimmune arthritis, J. Immunol., 184, 6882-6890, 2010.
- 30 Poppinger, D., Radom, L. and Pople, J. A.: A theoretical study of the CHNO isomers, J. Am.
31 Chem. Soc., 99, 7806-7816, 1977.
- 32 Rabalais, J. W., McDonald, J. R. and McGlynn, S. P.: Electronic states of HNCO, cyanate
33 salts, and organic isocyanates. II. Absorption studies, J. Chem. Phys., 51, 5103-5111,
34 <http://dx.doi.org/10.1063/1.1671908>, 1969.

- 1 Roberts, J. M., Veres, P., Warneke, C., Neuman, J. A., Washenfelder, R. A., Brown, S. S.,
2 Baasandorj, M., Burkholder, J. B., Burling, I. R., Johnson, T. J., Yokelson, R. J. and de
3 Gouw, J.: Measurement of HONO, HNCO, and other inorganic acids by negative-ion proton-
4 transfer chemical-ionization mass spectrometry (NI-PT-CIMS): application to biomass
5 burning emissions, *Atmos. Meas. Tech.*, 3, 981-990, 2010.
- 6 Roberts, J. M.: Measurement of the Henry's law coefficient and first order loss rate of PAN in
7 n-octanol, *Geophys. Res. Lett.*, 32, L08803, 2005.
- 8 Roberts, J. M., Veres, P. R., Cochran, A. K., Warneke, C., Burling, I. R., Yokelson, R. J.,
9 Lerner, B., Gilman, J. B., Kuster, W. C., Fall, R. and de Gouw, J.: Isocyanic acid in the
10 atmosphere and its possible link to smoke-related health effects, *Proc. Natl. Acad. Sci. U. S.*
11 *A.*, 108, 8966-8971, 10.1073/pnas.1103352108, 2011.
- 12 Roberts, J. M., Veres, P. R., VandenBoer, T. C., Warneke, C., Graus, M., Williams, E. J.,
13 Lefer, B., Brock, C. A., Bahreini, R., Öztürk, F., Middlebrook, A. M., Wagner, N. L., Dubé,
14 W. P. and de Gouw, J. A.: New insights into atmospheric sources and sinks of isocyanic acid,
15 HNCO, from recent urban and regional observations, *J. Geophys. Res. Atmos.*,
16 2013JD019931, 2014.
- 17 Sander, R.: Compilation of Henry's law constants (version 4.0) for water as solvent, *Atmos.*
18 *Chem. Phys.*, 15, 4399-4981, 2015.
- 19 Sander, R.: Modeling atmospheric chemistry: interactions between gas-phase species and
20 liquid cloud/aerosol particles, *Surv. Geophys.*, 20, 1-31, 1999.
- 21 Tsang, W.: Chemical kinetic data base for propellant combustion. II. Reactions involving CN,
22 NCO, and HNCO, *J. Phys. Chem. Ref. Data*, 21, 753-791,
23 <http://dx.doi.org/10.1063/1.555914>, 1992.
- 24 Tully, F. P., Perry, R. A., Thorne, L. R. and Allendorf, M. D.: Free-radical oxidation of
25 isocyanic acid, *Symp. Int. Combust.*, 22, 1101-1106, 1989.
- 26 Veres, P., Roberts, J. M., Burling, I. R., Warneke, C., de Gouw, J. and Yokelson, R. J.:
27 Measurements of gas-phase inorganic and organic acids from biomass fires by negative-ion
28 proton-transfer chemical-ionization mass spectrometry, *J. Geophys. Res.*, 115, D23302, 2010.
- 29 Veres, P., Roberts, J. M., Warneke, C., Welsh-Bon, D., Zahniser, M., Herndon, S., Fall, R.
30 and de Gouw, J.: Development of negative-ion proton-transfer chemical-ionization mass
31 spectrometry (NI-PT-CIMS) for the measurement of gas-phase organic acids in the
32 atmosphere, *Int. J. Mass Spectrom.*, 274, 48-55, 2008.
- 33 Wang, Z., Nicholls, S. J., Rodriguez, E. R., Kummu, O., Horkko, S., Barnard, J., Reynolds,
34 W. F., Topol, E. J., DiDonato, J. A. and Hazen, S. L.: Protein carbamylation links
35 inflammation, smoking, uremia and atherogenesis, *Nat. Med.*, 13, 1176-1184, 2007.
- 36 Wentzell, J. J. B., Liggio, J., Li, S., Vlasenko, A., Staebler, R., Lu, G., Poitras, M., Chan, T.
37 and Brook, J. R.: Measurements of gas phase acids in diesel exhaust: a relevant source of
38 HNCO?, *Environ. Sci. Technol.*, 47, 7663-7671, 2013.

- 1 Woodward-Massey, R., Taha, Y. M., Moussa, S. G. and Osthoff, H. D.: Comparison of
2 negative-ion proton-transfer with iodide ion chemical ionization mass spectrometry for
3 quantification of isocyanic acid in ambient air, *Atmos. Environ.*, 98, 693-703, 2014.
- 4 Young, P. J., Emmons, L. K., Roberts, J. M., Lamarque, J., Wiedinmyer, C., Veres, P. and
5 VandenBoer, T. C.: Isocyanic acid in a global chemistry transport model: tropospheric
6 distribution, budget, and identification of regions with potential health impacts, *J. Geophys.*
7 *Res.*, 117, D10308, 2012.
- 8 Yu, S., Su, S., Dorenkamp, Y., Wodtke, A. M., Dai, D., Yuan, K. and Yang, X.: Competition
9 between direct and indirect dissociation pathways in ultraviolet photodissociation of HNCO,
10 *J. Phys. Chem. A*, 117, 11673-11678, 2013.
- 11 Zhao, R., Lee, A. K. Y., Wentzell, J. J. B., McDonald, A. M., Toom-Sauntry, D., Leitch, W.
12 R., Modini, R. L., Corrigan, A. L., Russell, L. M., Noone, K. J., Schroder, J. C., Bertram, A.
13 K., Hawkins, L. N., Abbatt, J. P. D. and Liggio, J.: Cloud partitioning of isocyanic acid
14 (HNCO) and evidence of secondary source of HNCO in ambient air, *Geophys. Res. Lett.*, 41,
15 6962-6969, 2014.
- 16